

Resonant enhancement of thermoelectric properties by correlated hopping for the Falicov-Kimball model on Bethe lattice

D. A. Dobushovskiy and A. M. Shvaika

Institute for Condensed Matter Physics of the National Academy of Sciences of Ukraine, Lviv 79011, Ukraine

V. Zlatić

*Institute of Physics, Zagreb POB 304, Croatia**and Department of Physics, Faculty of Science, University of Split, HR-21000 Split, Croatia*

(Received 23 September 2016; revised manuscript received 29 January 2017; published 27 March 2017)

The effect of correlated hopping on the charge and heat transport of strongly correlated particles is studied for the Falicov-Kimball model on the Bethe lattice. Exact solutions for the one-particle density of states (DOS) and two-particle transport function (the “quasiparticle” scattering time) are derived using dynamical mean-field theory. For a wide range of the correlated hopping, the transport function exhibits singularities due to the resonant two-particle contribution, whereas the one-particle DOS does not show any anomalous features. By tuning the number of itinerant electrons, so as to bring the Fermi level close to the resonant frequency, we get a large increase of the electrical and thermal conductivities, and the thermoelectric power. When the hopping amplitude between the occupied sites is reduced sufficiently, the itinerant electrons localize in the clusters of sites occupied by f electrons. This gives rise to an additional narrow band in the DOS between the lower and upper Hubbard bands but has only a minor effect on the thermoelectric properties.

DOI: [10.1103/PhysRevB.95.125133](https://doi.org/10.1103/PhysRevB.95.125133)

I. INTRODUCTION

The effects of electron correlations on various phenomena in different materials, from the one- and two-dimensional organic conductors, through three-dimensional solids, up to the optical lattices, have been attracting considerable interest for more than half a century. The majority of publications dealing with these problems considered only the local Coulomb correlations of the Hubbard or Anderson type, $U \sum_i \hat{n}_{i\uparrow} \hat{n}_{i\downarrow}$. However, as noticed by Hubbard in his seminal article [1], the second quantized representation of the interelectron Coulomb interaction should also take into account, besides the local term, the nonlocal contributions. He pointed to the intersite Coulomb interaction $\sum_{ij} V_{ij} \hat{n}_i \hat{n}_j$ and the so-called correlated hopping,

$$\sum_{ij\sigma} t_{ij}^{(2)} (\hat{n}_{i\bar{\sigma}} + \hat{n}_{j\bar{\sigma}}) c_{i\sigma}^\dagger c_{j\sigma}, \quad (1)$$

which reflects the fact that the overlap of different many-body states is not the same, so that the value of intersite hopping depends on the occupation of these states. The origin of the correlated hopping can be either a direct intersite interaction or an indirect effective one [2,3], which can produce the multiparticle interactions, e.g., the three-particle one $\sum_{ij\sigma} t_{ij}^{(3)} \hat{n}_{i\bar{\sigma}} c_{i\sigma}^\dagger c_{j\sigma} \hat{n}_{j\bar{\sigma}}$.

While the effects of local Coulomb interaction described by the Hubbard and Anderson models have widely been investigated in the theory of strongly correlated electron systems, correlated hopping has attracted much less attention.¹

It was considered in connection with the new mechanisms for high-temperature superconductivity [5,6], properties of organic compounds [7] and molecular crystals [8], electron-hole asymmetry [9], and enhancement of magnetic properties [10]. Recently, correlated hopping has been examined in relation to quantum dots [11–13] and fermionic [14,15] and bosonic [16–18] atoms on optical lattices. However, due to its nonlocal character, the theoretical treatment of correlated hopping is difficult and, in most cases, the solutions can only be obtained by rather drastic approximations.

The exact results, that one can obtain in some special cases, are of great importance, as they can be used for benchmarking various approximations. Here, we study the effects of correlated hopping using the Falicov-Kimball model, the simplest model of strongly correlated electrons [19]. In its canonical form, it considers the local interaction between the itinerant d electrons and localized f electrons. It is a binary-alloy-type model and its ground-state phase diagram for the one-dimensional ($D = 1$) and two-dimensional ($D = 2$) cases displays a variety of modulated phases [20–23]. The dynamical mean-field theory (DMFT) [24–26] yields an exact solution of the Falicov-Kimball model in infinite dimensions, based on which the phase diagram and phase transitions in ordered phase were investigated and different spectral functions and responses were calculated [27]. An extension of the model, so as to include the correlated hopping, was also considered and the DMFT solution with a nonlocal self-energy was obtained [28–30].

In this article we study the effect of correlated hopping on the charge and heat transport of the Falicov-Kimball model on the Bethe lattice. The correlated hopping makes

¹The name used for such contributions is not well established yet. Apart from the term “correlated hopping,” many other terms circulate, such as “assisted hopping,” “bond-charge interaction (repulsion),” “occupation-dependent hopping,” “correlated hybridization,” etc.

Similar contributions in the theory of disordered systems are also known as an “off-diagonal disorder” [4].

the Falicov-Kimball model similar to the binary alloy model with off-diagonal disorder [4], studied long ago by Hoshino and Niizeki [31]. Using the Mott's relation and considering the special case of the hopping matrix with zero determinant [32] (see below) they obtained the thermoelectric power of the model. More recently [33], the general case of the hopping matrix was addressed on a $D \rightarrow \infty$ hypercubic lattice with the Gaussian density of states (DOS). Unfortunately, in this case one encounters several difficulties related to an infinite bandwidth and a finite “quasiparticle” scattering time at $\omega \rightarrow \pm\infty$ [34]. In the case of a Bethe lattice with a semielliptic density of states, the bandwidth is finite and the “quasiparticle” scattering time vanishes whenever the DOS is zero, so one is closer to the three-dimensional systems [35]. Here, we calculate the single-particle and two-particle properties of an infinite-dimensional Falicov-Kimball model with correlated hopping and show that, unlike the single-particle DOS, the transport properties exhibit a number of surprising features. In infinite dimensions, the canonical model can have, at very low temperatures, a phase transition to an ordered phase. (For a Bethe lattice there are only two possibilities: two-sublattice chessboard charge-density-wave ordering or segregation into two phases with different particle densities [36].) However, since the phase diagram for the model with correlated hopping is not known, we present the results for the homogeneous phase all the way down to $T = 0$.

The paper is organized as follows. In Sec. II, we present the DMFT solution for the Falicov-Kimball model with correlated hopping on a Bethe lattice. Section III provides the derivation of the charge and energy transport coefficients in a homogeneous phase. In Sec. IV, we consider peculiarities of the charge and heat transport for different values of the correlated hopping and doping. The results are summarized in Sec. V.

II. DMFT FORMALISM FOR CORRELATED HOPPING ON BETHE LATTICE

A. The model Hamiltonian

The Hamiltonian of the Falicov-Kimball model [19] with correlated hopping has the form

$$\begin{aligned} H &= H_{\text{loc}} + H_t, \\ H_{\text{loc}} &= \sum_i [U n_{id} n_{if} - \mu_f n_{if} - \mu_d n_{id}], \\ H_t &= \sum_{\langle ij \rangle} \frac{t_{ij}^*}{\sqrt{Z}} [t_1 d_i^\dagger d_j + t_2 d_i^\dagger d_j (n_{if} + n_{jf}) \\ &\quad + t_3 d_i^\dagger d_j n_{if} n_{jf}], \end{aligned} \quad (2)$$

where H_{loc} describes local correlations between the itinerant d electrons and localized f electrons, and H_t describes nonlocal terms on the Bethe lattice with infinite coordination number, $Z \rightarrow \infty$, including the nearest-neighbor intersite hopping with amplitude t_1 and nonlocal correlations with amplitudes t_2 and t_3 —the so-called correlated hopping. Because the number of localized particles is conserved, $[n_{if}, H] = 0$, one can introduce the projection operators $P_i^+ = n_{if}$ and

$P_i^- = 1 - n_{if}$, and define the projected d -electron operators

$$\mathbf{d}_i = \begin{pmatrix} d_i P_i^+ \\ d_i P_i^- \end{pmatrix}, \quad (3)$$

such that the nonlocal term assumes a matrix form [29],

$$\begin{aligned} H_t &= \sum_{\langle ij \rangle} \frac{t_{ij}^*}{\sqrt{Z}} [t^{++} P_i^+ d_i^\dagger d_j P_j^+ + t^{--} P_i^- d_i^\dagger d_j P_j^- \\ &\quad + t^{+-} P_i^+ d_i^\dagger d_j P_j^- + t^{-+} P_i^- d_i^\dagger d_j P_j^+] \\ &= \sum_{\langle ij \rangle} \frac{t_{ij}^*}{\sqrt{Z}} \mathbf{d}_i^\dagger \mathbf{t} \mathbf{d}_j. \end{aligned} \quad (4)$$

The hopping matrix is

$$\mathbf{t} = \begin{bmatrix} t^{++} & t^{+-} \\ t^{-+} & t^{--} \end{bmatrix}, \quad (5)$$

and the connection between its matrix elements and initial hopping amplitudes reads

$$\begin{aligned} t^{--} &= t_1, & t_1 &= t^{--}, \\ t^{+-} &= t^{-+} = t_1 + t_2, & t_2 &= t^{+-(-+)} - t^{--}, \\ t^{++} &= t_1 + 2t_2 + t_3, & t_3 &= t^{++} + t^{--} - t^{+-} - t^{-+}. \end{aligned} \quad (6)$$

Our aim is to find the transport properties of the model which are related, for $Z \rightarrow \infty$, to the single-particle Green's function.

B. The single-particle Green's function

The off-diagonal Green's function for projected d electrons is defined by the matrix $\mathbf{G}_{ij} = [G_{ij}^{\alpha\beta}]$, where $\alpha, \beta = \pm$. On the imaginary time axis we have

$$\mathbf{G}_{ij}(\tau - \tau') = -\langle \mathcal{T} \mathbf{d}_i(\tau) \otimes \mathbf{d}_j^\dagger(\tau') \rangle, \quad (7)$$

where \mathcal{T} is the imaginary-time ordering operator, \otimes denotes the direct (Cartesian) product of two vectors, and the angular bracket denotes the quantum statistical averaging with respect to H . The Green's function is calculated by treating H_t as perturbation, i.e., by expanding around the atomic limit. This leads to the Dyson-type equation, which can be written in the matrix form as

$$\mathbf{G}_{ij}(\omega) = \mathbf{\Xi}_{ij}(\omega) + \sum_{\langle i'j' \rangle} \mathbf{\Xi}_{ij'}(\omega) \cdot \frac{t_{ji'}^*}{\sqrt{Z}} \mathbf{t} \cdot \mathbf{G}_{i'j}(\omega), \quad (8)$$

where $\mathbf{\Xi}_{ij}(\omega)$ is the irreducible cumulant [26,37], which cannot be split into two disconnected parts by removing a single hopping line.

In the $Z \rightarrow \infty$ limit, the irreducible cumulant is local [37],

$$\mathbf{\Xi}_{ij}(\omega) = \delta_{ij} \mathbf{\Xi}(\omega), \quad (9)$$

and can be computed by the DMFT. In that approach, the local Green's functions of the lattice is equated with the Green's functions of an auxiliary impurity embedded in a self-consistent bath, described by the time-dependent mean fields (λ fields). Introducing the unperturbed DOS of the Bethe

lattice,

$$\rho(\epsilon) = \frac{2}{\pi W^2} \sqrt{W^2 - \epsilon^2}, \quad (10)$$

we write the DMFT equation in the matrix form as [29]

$$\begin{aligned} \mathbf{G}_{\text{local}}(\omega) &\equiv \mathbf{G}_{ii}(\omega) = \int_{-\infty}^{+\infty} d\epsilon \rho(\epsilon) \mathbf{G}_{\epsilon}(\omega) \\ &= [\mathbf{\Xi}^{-1}(\omega) - \mathbf{\Lambda}(\omega)]^{-1} = \mathbf{G}_{\text{imp}}(\omega), \end{aligned} \quad (11)$$

where $\mathbf{\Lambda}(\omega) = [\lambda^{\alpha\beta}(\omega)]$ is the λ matrix, $\mathbf{G}_{\text{imp}}(\omega)$ is the Green's function for the auxiliary impurity problem, and

$$\mathbf{G}_{\epsilon}(\omega) = [\mathbf{\Xi}^{-1}(\omega) - \mathbf{t}\epsilon]^{-1} \quad (12)$$

is the lattice Green's function matrix with the components

$$G_{\epsilon}^{\beta\alpha}(\omega) = \frac{A_{\beta\alpha}(\omega) - B_{\beta\alpha}\epsilon}{C(\omega) - D(\omega)\epsilon + \epsilon^2 \det \mathbf{t}}. \quad (13)$$

Here, we introduced the matrix adjugate to $\mathbf{\Xi}^{-1}(\omega)$,

$$\mathbf{A}(\omega) = \text{adj } \mathbf{\Xi}^{-1}(\omega) = \mathbf{\Xi}(\omega) / \det \mathbf{\Xi}(\omega), \quad (14)$$

and the matrix adjugate of the hopping matrix \mathbf{t} ,

$$\mathbf{B} = \text{adj } \mathbf{t} = \mathbf{t}^{-1} \det \mathbf{t}. \quad (15)$$

For the 2×2 matrices, the scalars $C(\omega)$ and $D(\omega)$ are given by

$$C(\omega) = \det \mathbf{A}(\omega) = \det \mathbf{\Xi}^{-1}(\omega) = 1 / \det \mathbf{\Xi}(\omega) \quad (16)$$

and

$$D(\omega) = \text{Tr}[\mathbf{A}(\omega)\mathbf{t}] = \text{Tr}[\mathbf{\Xi}^{-1}(\omega)\mathbf{B}]. \quad (17)$$

The DMFT equation (11) contains two unknowns: the irreducible cumulant $\mathbf{\Xi}(\omega)$ and the dynamical mean field $\mathbf{\Lambda}(\omega)$, both of which are related to $\mathbf{G}_{\text{imp}}(\omega)$. The Green's function of the impurity model with correlated hopping is given by the exact expression

$$\begin{aligned} G_{\text{imp}}^{++}(\omega) &= w_1 g_1(\omega), \\ G_{\text{imp}}^{--}(\omega) &= w_0 g_0(\omega), \\ G_{\text{imp}}^{+-}(\omega) &= G_{\text{imp}}^{-+}(\omega) = 0, \end{aligned} \quad (18)$$

where $w_1 = \langle P^+ \rangle = \langle n_f \rangle$, $w_0 = \langle P^- \rangle = \langle 1 - n_f \rangle$, and

$$\begin{aligned} g_0(\omega) &= \frac{1}{\omega + \mu_d - \lambda^{--}(\omega)} \\ g_1(\omega) &= \frac{1}{\omega + \mu_d - U - \lambda^{++}(\omega)} \end{aligned} \quad (19)$$

are the impurity Green's functions of a conduction electron in the presence of an f state which is either permanently empty or occupied (i.e., locators in the CPA theory [4]). The impurity Green's function yields the renormalized DOS of the lattice,

$$\begin{aligned} A_d(\omega) &= -\frac{1}{\pi} \sum_{\alpha, \beta=\pm} \text{Im } G_{\text{imp}}^{\alpha\beta}(\omega) \\ &= -\frac{1}{\pi} [w_0 \text{Im } g_0(\omega) + w_1 \text{Im } g_1(\omega)], \end{aligned} \quad (20)$$

and, for the Bethe lattice, we can write the DMFT equation (11) as [29]

$$\mathbf{\Lambda}(\omega) = \frac{W^2}{4} \mathbf{t} \mathbf{G}_{\text{imp}}(\omega) \mathbf{t}. \quad (21)$$

In numerical calculations, we use $W = 2$, which defines our energy scale. Equation (19) allows us to express the diagonal components of the $\mathbf{\Lambda}$ matrix in Eq. (21) in terms of g_0 and g_1 , and write the system of equations

$$\begin{aligned} \omega + \mu_d - U - \frac{1}{g_1(\omega)} &= \frac{W^2}{4} [(t^{++})^2 w_1 g_1(\omega) + (t^{+-})^2 w_0 g_0(\omega)], \\ \omega + \mu_d - \frac{1}{g_0(\omega)} &= \frac{W^2}{4} [(t^{+-})^2 w_1 g_1(\omega) + (t^{--})^2 w_0 g_0(\omega)], \end{aligned} \quad (22)$$

which, in general, provides the fourth-order polynomial equations for $g_0(\omega)$ or $g_1(\omega)$.

Previous investigations of the Falicov-Kimball model with correlated hopping [29,33] have shown that the renormalized DOS and transport properties depend strongly on the structure of the hopping matrix (5), and that one can distinguish five different cases (in what follows, unless stated explicitly, we take $t^{--} = t_1 = 1$):

(a) For $t^{++} \neq 0$, $t^{+-} \neq 0$, and $\det \mathbf{t} = 0$, the right-hand parts of Eqs. (22) are proportional to each other, so that

$$\begin{aligned} \frac{1}{t^{++}} \left[\omega + \mu_d - U - \frac{1}{g_1(\omega)} \right] &= \frac{1}{t^{--}} \left[\omega + \mu_d - \frac{1}{g_0(\omega)} \right] \\ &= \frac{W^2}{4} [t^{++} w_1 g_1(\omega) + t^{--} w_0 g_0(\omega)]. \end{aligned} \quad (23)$$

This case was considered by Shiba [32] and Hoshino and Niizeki [31]. The regular Falicov-Kimball model, without the correlated hopping, belongs also to this case.

(b) For $t^{++} = 0$, $t^{+-} \neq 0$, and $\det \mathbf{t} \neq 0$, one of the diagonal components of the hopping matrix vanishes, so that the direct hopping of d particles between the sites occupied by the f particles is reduced.

(c) For $t^{++} \neq 0$, $t^{+-} = 0$, and $\det \mathbf{t} \neq 0$, the hopping matrix is diagonal and the hopping of d particles is allowed only between the sites with the same occupation of f states.

(d) For $t^{++} = 0$, $t^{+-} = 0$, and $\det \mathbf{t} = 0$ we are dealing with the simultaneous realization of all three previous cases, and the hopping of d particles is allowed only between the sites which are *not* occupied by the f particles.

(e) The most general case is obtained for $t^{++} \neq 0$, $t^{+-} \neq 0$, $\det \mathbf{t} \neq 0$.

For the cases (a,b) and (c,d), the impurity Green's functions $g_0(\omega)$ or $g_1(\omega)$ are defined by the cubic and quadratic equations, respectively. Within the solutions of these equations, we choose the one with negative imaginary parts, which yields the retarded Green's functions. For the general case (e), the quartic polynomial equation with real coefficients has either four real roots, or two real and two mutually conjugated complex roots,

or two pairs of mutually conjugated complex roots. The correct physical solution is the one with negative imaginary parts, which gives the retarded Green's functions $g_0(\omega)$ and $g_1(\omega)$. It can be shown that there is always just a single set of physical solutions. When ω has only the real roots, the physical solution is obtained by using the spectral relation

$$\text{Re } g_{0,1}(\omega) = -\frac{1}{\pi} \int_{-\infty}^{+\infty} d\omega' \frac{\text{Im } g_{0,1}(\omega')}{\omega - \omega'}, \quad (24)$$

which yields the correct retarded Green's functions and renormalized single-particle density of states.

For the local single-particle Green's function

$$G_{ii}(\tau - \tau') = -\langle \mathcal{T} d_i(\tau) d_i^\dagger(\tau') \rangle, \quad (25)$$

we have

$$\begin{aligned} G_{ii}(\omega) &= \sum_{\alpha, \beta = \pm} G_{\text{imp}}^{\alpha\beta}(\omega) = w_0 g_0(\omega) + w_1 g_1(\omega) \\ &= [\omega + \mu_d - \Sigma(\omega) - \lambda_{\text{HF}}(\omega)]^{-1}, \end{aligned} \quad (26)$$

where $\lambda_{\text{HF}}(\omega) = w_1 \lambda^{++}(\omega) + w_0 \lambda^{--}(\omega)$ is the Hartree-Fock dynamical mean field and

$$\Sigma(\omega) = U w_1 + \frac{\tilde{U}^2(\omega) w_1 w_0}{\omega + \mu_d - \tilde{U}(\omega) w_0 - \lambda^{--}(\omega)} \quad (27)$$

is local self-energy, which is different from the nonlocal one for the lattice Green's function [29]. The parameter

$$\tilde{U}(\omega) = U + \lambda^{++}(\omega) - \lambda^{--}(\omega) \quad (28)$$

is an effective retarded Coulomb interaction. These expressions reveal the dual nature of correlated hopping: on one hand, it modifies the hopping amplitude in the Hartree-Fock term $\lambda_{\text{HF}}(\omega)$, and, on the other hand, it leads to the nonlocal two-particle correlation, which gives rise to the retarded local interaction.

For a given value of the d -electron concentration, $n_d = \langle n_d \rangle$, the chemical potential μ_d is obtained by solving the equation

$$n_d = -\frac{1}{\pi} \int_{-\infty}^{+\infty} d\omega f(\omega) \text{Im } G_{ii}(\omega), \quad (29)$$

where $f(\omega) = 1/(e^{\omega/T} + 1)$ is the Fermi function and $G_{ii}(\omega)$ is given by Eq. (26).

III. TRANSPORT COEFFICIENTS IN THE PRESENCE OF CORRELATED HOPPING

We now calculate the transport properties of correlated electrons by linear response theory. The Falicov-Kimball model with correlated hopping satisfies the Boltzmann (Jonson-Mahan) theorem [33,38–40] so that all transport integrals follow from a single transport function,

$$\mathbf{L}_{lm} = \frac{\sigma_0}{e^2} \int_{-\infty}^{+\infty} d\omega \left[-\frac{df(\omega)}{d\omega} \right] \mathbf{I}(\omega) \omega^{l+m-2}, \quad (30)$$

where $\mathbf{I}(\omega)$ is the transport function, which is given below.

The dc charge conductivity σ_{dc} , the Seebeck coefficient (thermoelectric power $\mathbf{E} = \mathbf{S} \nabla T$), and the electronic contribution to thermal conductivity κ_e follow immediately from the

transport integrals as

$$\sigma_{\text{dc}} = e^2 \mathbf{L}_{11}, \quad (31)$$

$$\mathbf{S} = \frac{1}{eT} \mathbf{L}_{11}^{-1} \mathbf{L}_{12}, \quad (32)$$

$$\kappa_e = \frac{1}{T} [\mathbf{L}_{22} - \mathbf{L}_{21} \mathbf{L}_{11}^{-1} \mathbf{L}_{12}]. \quad (33)$$

The DMFT expression for transport function, generalized to the case of correlated hopping, reads

$$\begin{aligned} I(\omega) &= \frac{1}{\pi} \int d\epsilon \rho(\epsilon) \Phi_{xx}(\epsilon) \text{Tr} [\mathbf{t} \text{Im } \mathbf{G}_\epsilon(\omega) \mathbf{t} \text{Im } \mathbf{G}_\epsilon(\omega)] \\ &= \frac{1}{\pi} \sum_{\alpha\beta\alpha'\beta'} t^{\alpha\beta} t^{\alpha'\beta'} \int d\epsilon \rho(\epsilon) \Phi_{xx}(\epsilon) \text{Im } G_\epsilon^{\beta\alpha'}(\omega) \text{Im } G_\epsilon^{\beta'\alpha}(\omega), \end{aligned} \quad (34)$$

where $\Phi_{xx}(\epsilon)$ is the so-called lattice-specific transport DOS [41]. For a $D = \infty$ hypercubic lattice with Gaussian DOS, we have $\Phi_{xx}(\epsilon) = W^2/2D$, whereas for the $Z = \infty$ Bethe lattice with semielliptic DOS, the f -sum rule yields [42]

$$\Phi_{xx}(\epsilon) = \frac{1}{3Z} (W^2 - \epsilon^2). \quad (35)$$

The integral over ϵ in Eq. (34) can now be evaluated and we find that the final result depends on the value of $\det \mathbf{t}$.

For $\det \mathbf{t} = 0$, we find

$$I(\omega) = \frac{1}{2\pi} \left\{ \text{Re } \Psi' \left[\frac{C(\omega)}{D(\omega)} \right] - \frac{\text{Im } \Psi \left[\frac{C(\omega)}{D(\omega)} \right]}{\text{Im} \left[\frac{C(\omega)}{D(\omega)} \right]} \right\}, \quad (36)$$

where

$$\begin{aligned} \Psi(\zeta) &= \int d\epsilon \frac{\rho(\epsilon)}{\zeta - \epsilon} \Phi_{xx}(\epsilon), \\ \Psi'(\zeta) &= \frac{d\Psi(\zeta)}{d\zeta}. \end{aligned} \quad (37)$$

For the semielliptic DOS, we find

$$\begin{aligned} \Psi(\zeta) &= \frac{1}{3} [(W^2 - \zeta^2) F(\zeta) + \zeta], \\ \Psi'(\zeta) &= \frac{1}{3} [(W^2 - \zeta^2) F'(\zeta) + 1 - 2\zeta F(\zeta)], \end{aligned} \quad (38)$$

where

$$\begin{aligned} F(\zeta) &= \int d\epsilon \frac{\rho(\epsilon)}{\zeta - \epsilon} = \frac{2}{W^2} (\zeta - \sqrt{\zeta^2 - W^2}), \\ F'(\zeta) &= \frac{dF(\zeta)}{d\zeta} = \frac{\zeta F(\zeta) - 2}{\zeta^2 - W^2}. \end{aligned} \quad (39)$$

The transport function (36) is similar to the one for the Falicov-Kimball model without correlated hopping, provided we replace the inverse irreducible cumulant $\Xi^{-1}(\omega) = \omega + \mu_d - \Sigma(\omega)$ by the expression

$$\frac{C(\omega)}{D(\omega)} = \frac{1}{\text{Tr} [\Xi(\omega) \mathbf{t}]} \quad (40)$$

For $\det \mathbf{t} \neq 0$, the transport function reads

$$I(\omega) = \frac{1}{2\pi} \left[\text{Re} \{ \Psi' [E_1(\omega)] + \Psi' [E_2(\omega)] \} - \frac{\text{Im} \Psi [E_1(\omega)]}{\text{Im} E_1(\omega)} - \frac{\text{Im} \Psi [E_2(\omega)]}{\text{Im} E_2(\omega)} - K(\omega) \left\{ \frac{1}{\text{Im} E_1(\omega)} \text{Im} \frac{\Psi [E_1(\omega)]}{[E_1(\omega) - E_2(\omega)][E_1(\omega) - E_2^*(\omega)]} + \frac{1}{\text{Im} E_2(\omega)} \text{Im} \frac{\Psi [E_2(\omega)]}{[E_2(\omega) - E_1(\omega)][E_2(\omega) - E_1^*(\omega)]} \right\} \right], \quad (41)$$

where E_1 and E_2 are the roots of the denominator in Eq. (13), $C(\omega) - D(\omega)\epsilon + \epsilon^2 \det \mathbf{t} = 0$, given by

$$E_1(\omega) = \frac{D(\omega)}{2 \det \mathbf{t}} \left[1 + \sqrt{1 - \frac{4C(\omega)}{D^2(\omega)} \det \mathbf{t}} \right], \quad (42)$$

$$E_2(\omega) = \frac{2C(\omega)}{D(\omega)} \left[1 + \sqrt{1 - \frac{4C(\omega)}{D^2(\omega)} \det \mathbf{t}} \right]^{-1}, \quad (43)$$

and $K(\omega)$ reads

$$K(\omega) = 2 \text{Re} [E_1(\omega) E_2^*(\omega)] - \frac{1}{\det \mathbf{t}} \text{Re} \text{Tr} [\mathbf{A}^*(\omega) \mathbf{\Xi}^{-1}(\omega)]. \quad (44)$$

In the limit $\det \mathbf{t} \rightarrow 0$, the eigenvalue E_1 diverges and its contribution to the transport function vanishes, whereas $E_2(\omega) \rightarrow C(\omega)/D(\omega)$, so that we recover the transport function given by expression (36).

IV. RESULTS

In the first part of this section we show how the interacting density of states $A_d(\omega)$ and transport function $I(\omega)$ depend on frequency ω and correlated hopping t_2 . The functional form of both functions changes with the concentration of f electrons $n_f = \langle n_f \rangle$ but does not depend on the chemical potential of d particles μ_d . Thus, we plot $A_d(\omega)$ and $I(\omega)$ with $\omega + \mu_d$ on the abscissa. Furthermore, since t_2 and t_3 enter all the expressions only through the matrix elements $t^{\alpha\beta}$ defined in Eq. (5), we show the results for $t_3 = 0$ only. Finite values of t_3 can change the results in a quantitative but not in a qualitative way. The data are presented for various concentrations of f particles, in the weak ($U = 0.25$) and the strong ($U = 2$) coupling regime. In the second part of this section, we discuss the effect of correlated hopping on $A_d(\omega)$ and $I(\omega)$, for typical values of the parameters, and show the corresponding transport coefficients in the weak- and strong-coupling limit.

A. Overall features of the DOS and transport function

The dependence of $A_d(\omega)$ and $I(\omega)$ on $\omega + \mu_d$ and t_2 is shown in Fig. 1 on a false color plot, for $n_f = 0.5, 0.75$, and 0.9 , in the weak-coupling limit ($U = 0.25$, $t_3 = 0$). The data show that $A_d(\omega)$ and $I(\omega)$ have the same bandwidth,

which increases for $t_2 > 0$ and $t_2 < -1$, while it shrinks for $-1 < t_2 < 0$.

The DOS is a smooth and almost semielliptic function for all values of t_2 , except for $t_2 \approx -(t_1 + t_3)/2 \approx -0.5$, where the matrix element t^{++} is small and changes sign. At half filling, $n_f = 0.5$, and in the vicinity of $t_2 = -0.5$ ($t^{++} = 0$), the DOS exhibits a tiny gap at $\omega + \mu_d = U$ [see insert in Fig. 1(a)], with a sharp peak at the bottom edge of the upper band [see Fig. 7 below]. For larger values of n_f , the DOS develops more prominent gaps, generating, first, a two-band and, then, a three-band structure. In the case of the two-band structure, the spectral weights of the lower and upper bands are $w_0 = 1 - n_f$ and $w_1 = n_f$, respectively, which is similar to what one finds in the doped Mott-Hubbard insulator phase of the Falicov-Kimball model without correlated hopping [35,43,44]. As we approach the $t^{++} = 0$ point, an additional gap appears in the upper Hubbard band and the two-peak structure is transformed into a three-peak one; the spectral weights of the lower and upper bands are the same, $w_0 = 1 - n_f$, while the spectral weight of the middle band is $2n_f - 1$. For $t^{++} \rightarrow 0$, the DOS of the middle band narrows to a δ peak.

The midband emerges, for $n_f > 1/2$, because the probability of the neighboring sites being occupied by the f particles becomes macroscopically large so that the clusters of sites occupied by the f particles are created. Since the value of t_2 is such that the hopping matrix element t^{++} is very small, a direct hopping of d particles between these sites is suppressed. Thus, the d particles within the cluster are localized and we observe a band of localized states which are separated from the upper Hubbard band by the localization gap. As $n_f \rightarrow 1$, almost all the sites are occupied by f particles, so that the cluster covers the whole lattice and the weight of the lower and upper band decreases as $1 - n_f$ and the DOS is dominated by a narrow peak of localized states located at $\omega + \mu_d = U$. The presence of the clusters of localized states strongly affects the properties of itinerant d electrons around the Fermi level E_F (the chemical potential μ_d at zero temperature). For $n_d < 1 - n_f$, the Fermi level is in the lower band; for $1 - n_f < n_d < n_f$, it is fixed in the narrow midpeak and the localized d states of clusters are filled; for $n_d > n_f$, the Fermi level is in the upper band.

In the strong-coupling limit, $A_d(\omega)$ and $I(\omega)$ change in a qualitative way. As shown in Fig. 2 (left panel), the Mott-Hubbard gap emerges now in an extended range of t_2 values, including the case without the correlated hopping (Mott transition in the regular Falicov-Kimball model). The localization band is pushed into the upper Hubbard band and is very narrow; the corresponding localization gap exists only in the immediate vicinity of the $t^{++} = 0$ value.

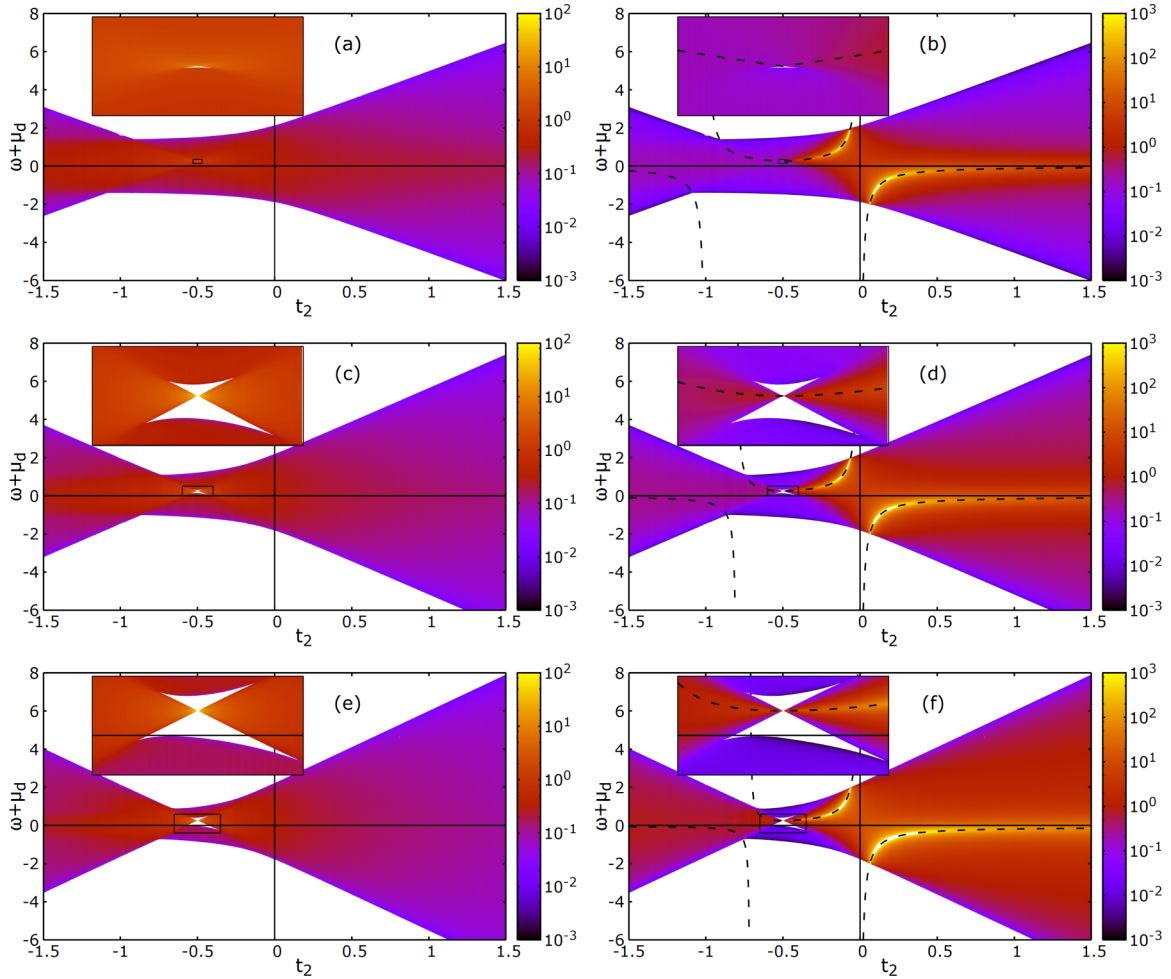


FIG. 1. The density of states $A_d(\omega)$, left panels (a), (c), (e), and transport function $I(\omega)$, right panels (b), (d), (f), shown as a function of frequency ω and correlated hopping parameter t_2 on a false color plot for $U = 0.25$, $t_3 = 0$, and for f -particle concentrations (a,b) $n_f = 0.5$, (c,d) 0.75 , and (e,f) 0.9 (top to bottom). Inserts represent enlarged rectangular areas with (a,b) $t_2 \in [-0.53, -0.47]$, $\omega + \mu_d \in [0.2, 0.3]$; (c,d) $t_2 \in [-0.6, -0.4]$, $\omega + \mu_d \in [0.0, 0.5]$; and (e,f) $t_2 \in [-0.65, -0.35]$, $\omega + \mu_d \in [-0.4, 0.6]$. Dashed line indicates the resonant frequency ω_{res} given by Eq. (46).

The above results show that the definition of the weak and strong coupling is modified by the dual nature of correlated hopping. Figures 1 and 2 indicate three regions of the parameter space with markedly different band structure. For large positive and negative t_2 , a single band, with a bandwidth which depends linearly on t_2 , is observed. Here, the amplitude of the Hartree-Fock hopping is larger than the effective Coulomb interaction, which is typical of a weak-coupling regime. The intermediate values of t_2 are characterized by a large reduction of the bandwidth and an opening of a band gap. The reduced amplitude of the Hartree-Fock hopping and the Mott-Hubbard gap are typical features of the strong-coupling regime. In the third case, for $t^{++} \simeq 0$, in addition to the Hubbard bands, there emerges a band of localized states.

The transport function, plotted in the right panel of Figs. 1 and 2, shows a completely different behavior than the density of states. For $t_2 > -(t_1 + t_3)/2$, and $t^{++} > 0$, $I(\omega)$ exhibits a large enhancement at a resonant frequency, $\omega = \omega_{\text{res}}$, which is indicated in Figs. 1 and 2 by dashed lines. Numerical analysis of Eq. (41) shows that the resonant contribution to $I(\omega)$ comes from the term $\text{Im} \Psi[E_2(\omega)]/\text{Im} E_2(\omega)$. At the resonance, the λ

fields and Green's functions satisfy the interference condition,

$$\frac{\lambda^{++}(\omega)}{\lambda^{--}(\omega)} = \frac{g_0(\omega)}{g_1(\omega)} = \eta, \quad (45)$$

which gives

$$\omega_{\text{res}} + \mu_d = \frac{U}{1 - \eta} \quad (46)$$

with

$$\eta = \frac{(t^{+-})^2}{(t^{--})^2} - \frac{(t^{+-})^2 - \sqrt{(t^{+-})^4 + 4w_1w_0[(t^{++}t^{--})^2 - (t^{+-})^4]}}{2(t^{--})^2w_0}. \quad (47)$$

For two special values of t_2 , given by the solutions of the equation $\eta = 1$ or

$$(t^{--})^2w_0 + (t^{+-})^2(w_1 - w_0) - (t^{++})^2w_1 = 0, \quad (48)$$

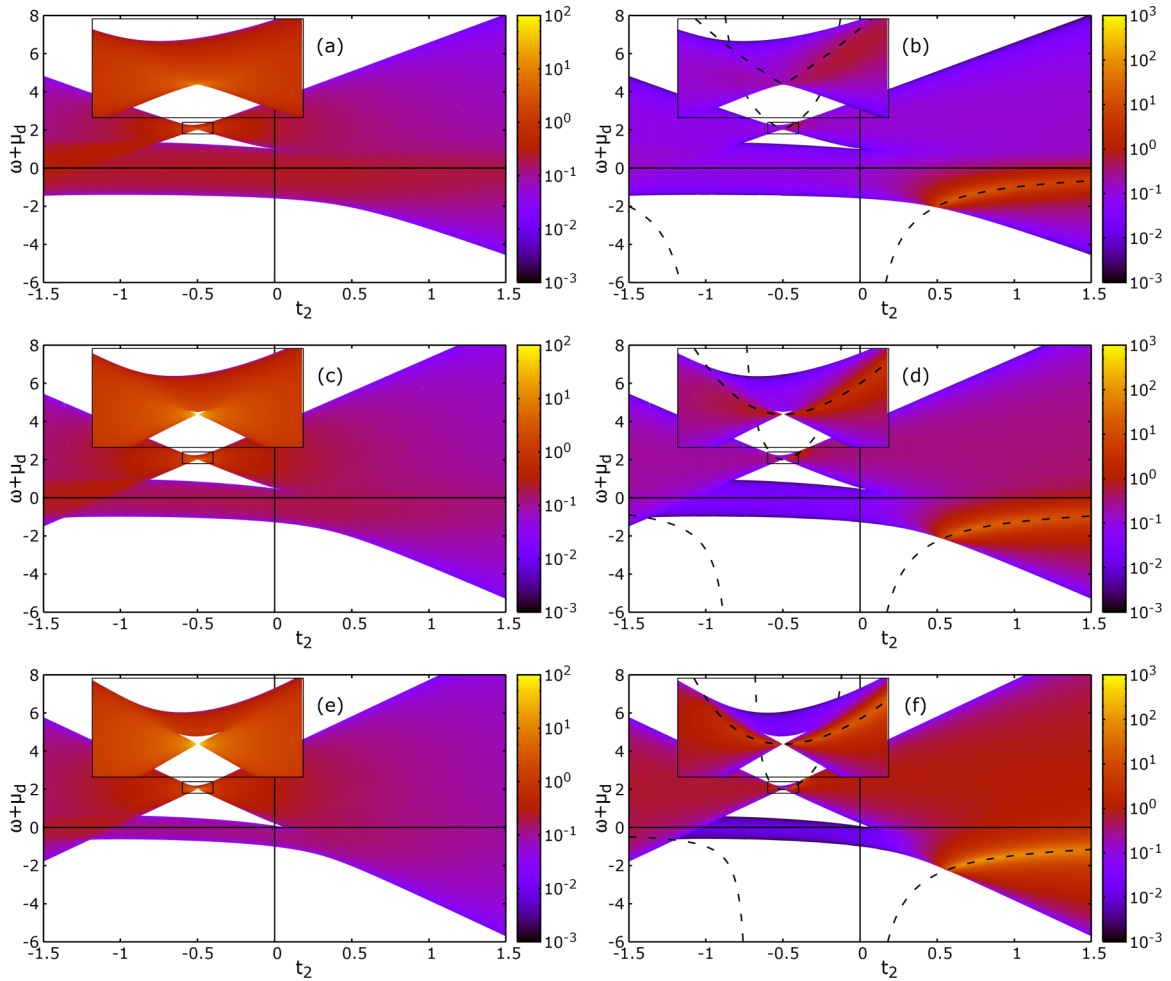


FIG. 2. Same as in Fig. 1 for $U = 2$. Inserts represent enlarged rectangular areas with $t_2 \in [-0.6, -0.4]$, $\omega + \mu_d \in [1.8, 2.4]$.

the resonant frequency is at infinity, i.e., it is shifted outside the bands. The regular Falicov-Kimball model, where $t^{--} = t^{+-} = t^{++} = t_1$, is precisely at one of these special points with $\omega_{\text{res}} \rightarrow \pm\infty$, so that the transport function has no resonant contribution. On the other hand, for $t^{++} \rightarrow 0$, ω_{res} is within the localized band and the resonant contributions become prominent for $t^{++} > 0$, while it is suppressed for $t^{++} < 0$.

Since the expressions given by Eqs. (46) and (47) for ω_{res} do not depend on the parameter W , characterizing the semielliptic DOS for the Bethe lattice, we conjecture that the same expressions also hold for other lattices with different unperturbed DOS. Direct numeric calculations for the hypercubic lattice with the Gaussian DOS confirm this conjecture but, in that case, there are no clear band edges and the resonant peak is within the band for any value of correlated hopping [33].

B. Transport coefficients

1. Weak-coupling regime

In the weak-coupling regime, the interaction constants are much smaller than the hopping integral: $|U|, |t_2|, |t_3| \ll |t_1|$. At half filling, $n_f = n_d = 1/2$, the renormalized DOS is slightly deformed with respect to the unperturbed semielliptic one, i.e., the correlated hopping breaks the electron-hole symmetry and makes $A_d(\omega)$ an asymmetric function [see Fig. 3(a)]. (At

half filling and without the correlated hopping, $t_2 = t_3 = 0$, the DOS is symmetric with respect to the frequency $\omega + \mu_d = U/2$.) The width of the conduction band increases for $t_2 > 0$ and decreases for $t_2 < 0$.

In contrast, the transport function $I(\omega)$, which is almost semielliptic in the absence of the correlated hopping, becomes highly asymmetric as soon as $t_2 \neq 0$. For $t_2 = \pm 0.05$, the resonant function is somewhat enhanced close to the band edges, but it is still smooth and almost flat around the chemical potential [see Fig. 3(b)]. Hence, the transport coefficients exhibit typical metallic behavior as functions of temperature (see Fig. 4). For $t_2 = \pm 0.1$, the resonant peak gives the main contribution to $I(\omega)$. At low temperatures, the resonant peak is outside the Fermi window, $-df(\omega)/d\omega|_{\omega \simeq \omega_{\text{res}}} \simeq 0$, and its contribution to the transport integrals is negligibly small. Hence, the transport coefficients exhibit a metallic behavior. However, as temperature increases, the resonant peaks enter the Fermi window and we observe, first, an enhancement of the thermal conductivity, then, of the thermoelectric power, and, eventually, of the electric conductivity (see Fig. 4).

Doping does not change much the shape of $A_d(\omega)$ and $I(\omega)$ in the weak-coupling regime, as shown by Fig. 5 for $n_f = 0.75$ and $n_d = 0.25$. The main effect is the shift of the chemical potential towards the bottom of the conduction band,

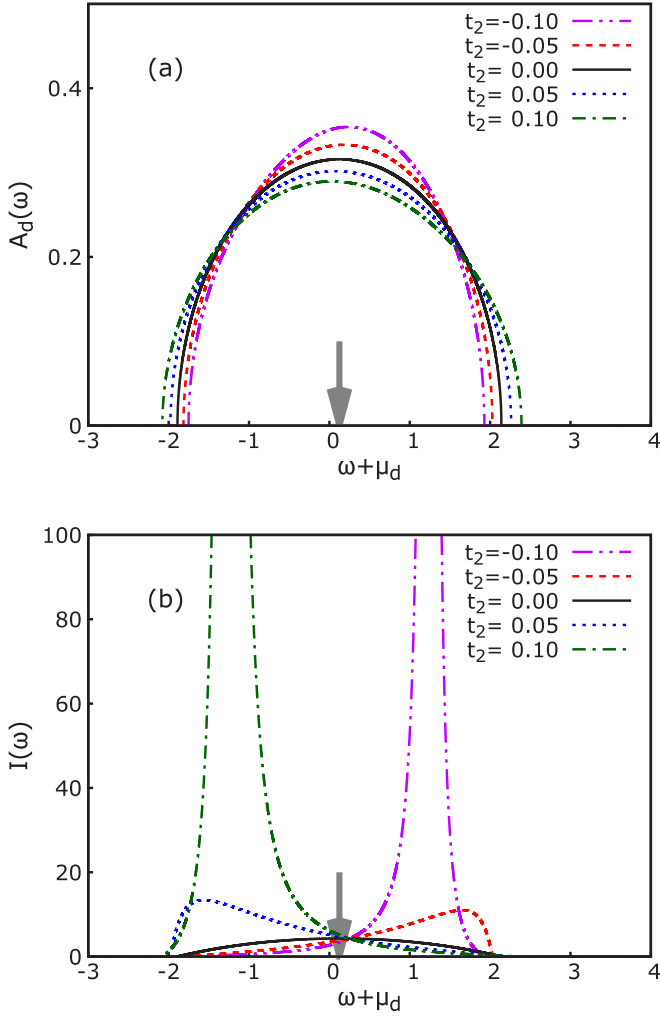


FIG. 3. The interacting DOS (panel a) and transport function (panel b) plotted versus frequency for $U = 0.25$ at half filling ($n_f = n_d = 1/2$) and for $t_2 = -0.1, -0.05, 0, 0.05, 0.1$ ($t_3 = 0$). The Fermi level E_F depends on the hopping t_2 , and the gray arrow indicates a narrow frequency interval in which E_F is located for different values of t_2 .

giving $\mu_d \approx -0.7$. For $t_2 = 0.1$, the resonant peak overlaps the Fermi level, so that the electric conductivity, the thermal conductivity, and the thermopower are enhanced with respect to the half-filled case and when the resonant peak is absent (see Fig. 6). For $t_2 = -0.1$, the resonant peak is too far away from the chemical potential to contribute to the electric and thermal conductivity, but a large asymmetry of $I(\omega)$, shown in Fig. 5(b), gives rise to an enhanced thermopower at high temperatures.

As shown in Fig. 2, an increase of local Coulomb interaction U shifts the resonant frequency in the region of large positive and negative values of t_2 , so that the resonant peaks do not affect much the transport properties for small values of correlated hopping t_2 . The only effect of correlated hopping is to break the electron-hole symmetry and to make $A_d(\omega)$ and $I(\omega)$ asymmetric functions of ω . Hence, in this part of the parameter space, the transport coefficients behave similarly as in the case of a doped Falicov-Kimball model without correlated hopping [35,43,44].

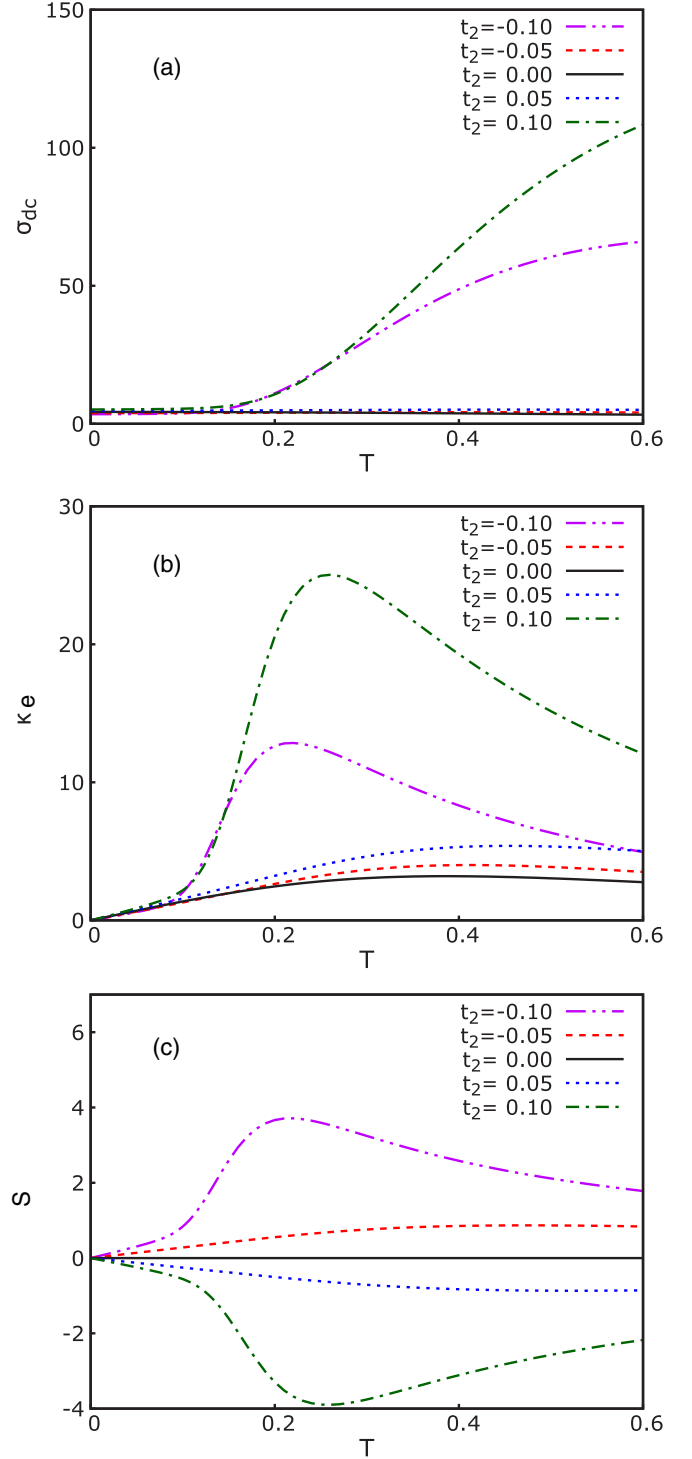


FIG. 4. Temperature dependences of the dc conductivity σ_{dc} , thermal conductivity κ_e , and Seebeck coefficient S for the same parameters as in Fig. 3.

A different behavior emerges for small values of t^{++} , when the direct hopping amplitude between the sites occupied by f particles is much reduced, while the hopping between occupied and unoccupied, and between the unoccupied sites is large. For the Gaussian density of states, this case was analyzed in Ref. [33] (see Figs. 6 and 7 of Ref. [33]). For the semielliptic

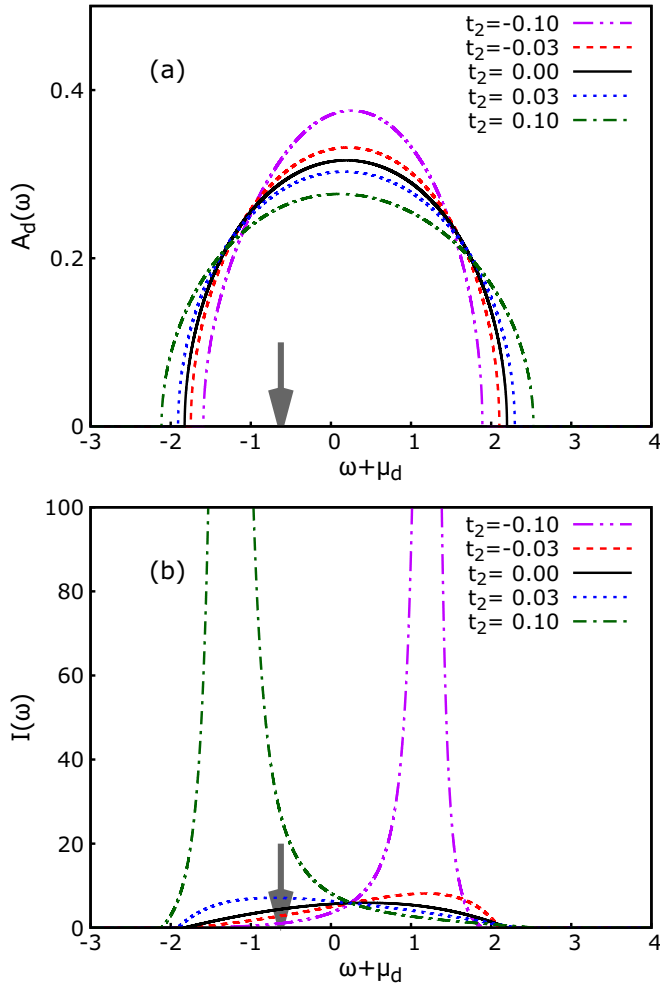


FIG. 5. The interacting DOS (panel a) and transport function (panel b) plotted versus frequency for $U = 0.25$, $n_f = 0.75$, and $n_d = 1 - n_f = 0.25$, and for $t_2 = -0.1, -0.03, 0, 0.03, 0.1$. The gray arrow indicates a narrow ω interval in which E_F is located for different values of t_2 .

density of states, we find similar behavior but the data reveal more details and we discover new interesting regimes, like the three-band structure in the DOS and the clusters of sites occupied by f electrons.

At half filling and $t^{++} = 0$ ($t_2 = -0.5$), the DOS acquires a tiny gap at the Fermi level, bounded by the singularity at the bottom of the upper Hubbard band [see Fig. 7(a)]. The transport function also displays a gap, but the band-edge singularity is replaced by a steplike function [Fig. 7(b)]. The presence of the gap at the Fermi level reduces the dc and thermal conductivities at low temperatures, whereas it increases the thermopower due to the asymmetry of $I(\omega)$ around the chemical potential (see Fig. 8). At high temperatures, when the width of the Fermi window exceeds the gap, the doped metallic or semiconductor behavior is restored.

At half filling and $t^{++} \neq 0$, the gap closes rapidly and the DOS exhibits a smooth peak around the chemical potential. For negative t^{++} ($t_2 < -0.5$), the transport function is smooth and we find a metallic behavior. For positive t^{++} ($t_2 > -0.5$), the transport function acquires a resonant peak such that the transport coefficients are enhanced at low temperatures (see Fig. 8).

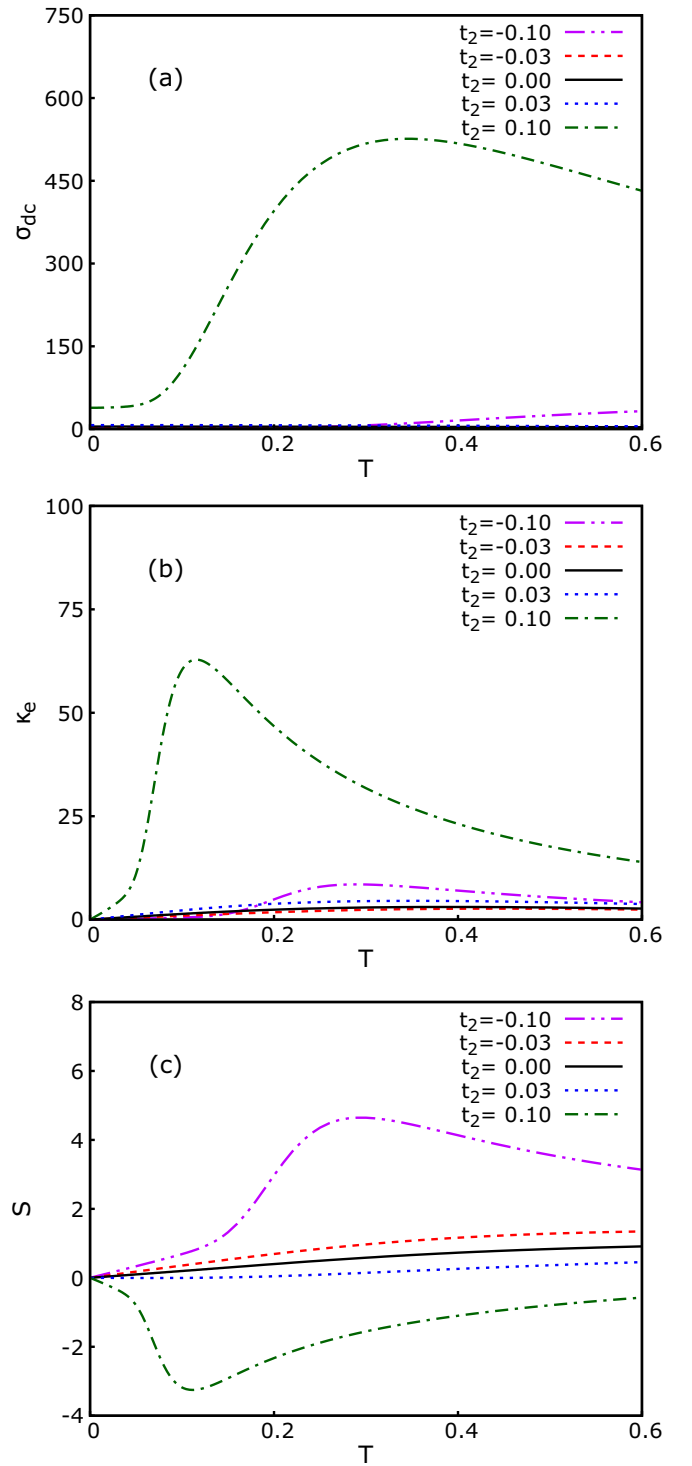


FIG. 6. Temperature dependences of the dc conductivity σ_{dc} , thermal conductivity κ_e , and Seebeck coefficient S are shown for the same parameters as in Fig. 5.

Away from half filling, the three-band structure of $A_d(\omega)$ emerges for small values of t^{++} . As shown in Fig. 9, for $t^{++} = 0$ ($t_2 = -0.5$) exactly, $A_d(\omega)$ exhibits two broad bands [the lower (1) and upper (2) Hubbard bands with spectral weights $1 - n_f$], and a δ peak (3) at $\omega + \mu_d = U$ with spectral weight $2n_f - 1$. The δ peak in $A_d(\omega)$ is due to the localized d states in the clusters of lattice sites occupied by f electrons. Because

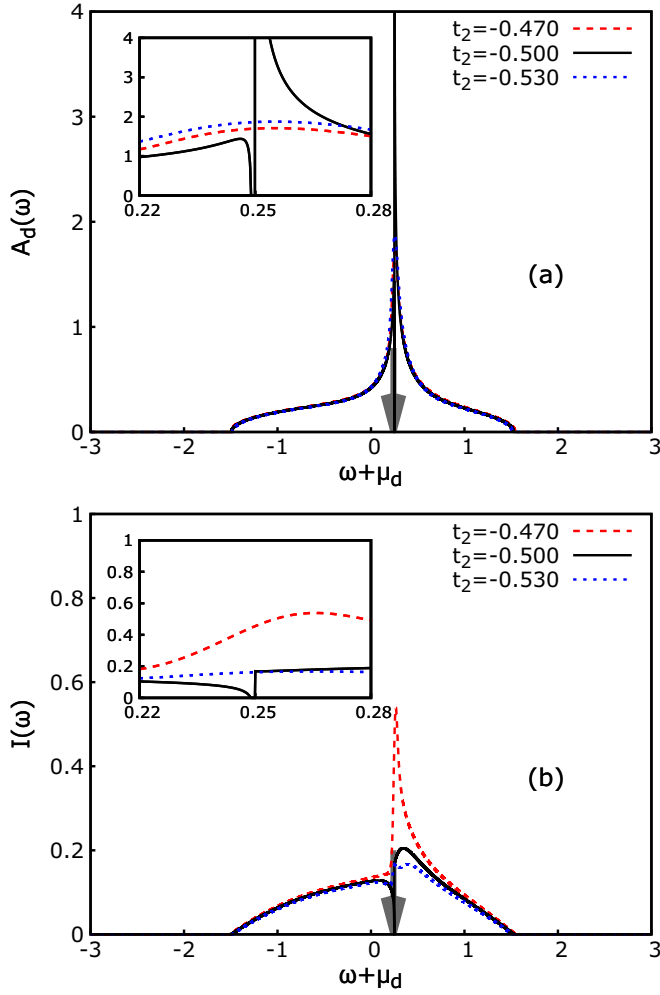


FIG. 7. The interacting DOS (panel a) and transport function (panel b) plotted versus ω for $U = 0.25$ at half filling ($n_f = n_d = 1/2$) and for $t_2 = -0.47, -0.5, -0.53$ ($t_3 = 0$). The gray arrow indicates a narrow ω interval in which E_F is located for different values of t_2 .

we have $n_d = 1 - n_f$, the Fermi level is in the gap between the lower Hubbard band and the localized band. Unlike the single-particle DOS, the transport function $I(\omega)$ has only two contributions, due to the lower and upper Hubbard band. The absence of any feature at $\omega + \mu_d = U$ is obvious. Since the localized states cannot contribute much to the charge or heat transport, the shape of $I(\omega)$ and temperature dependences of the transport coefficients (see Fig. 10) are similar to the one obtained for a doped Mott insulator [35,43,44].

Away from half filling and for $t^{++} \neq 0$ (Fig. 9), the δ peak of localized d states (3) broadens into a band which merges with the upper Hubbard band for larger values of $|t^{++}|$. The contribution of the localized state to transport function depends on the sign of t^{++} . For negative values of $t^{++} < 0$ ($t_2 < -0.5$), this contribution increases at first and, then, as t^{++} becomes more negative and the localized band merges with the upper Hubbard band, it decreases. For $t^{++} > 0$ ($t_2 > -0.5$), the resonant peak due to the localized states dominates the transport function. In both cases, the thermoelectric properties are enhanced, most prominently for

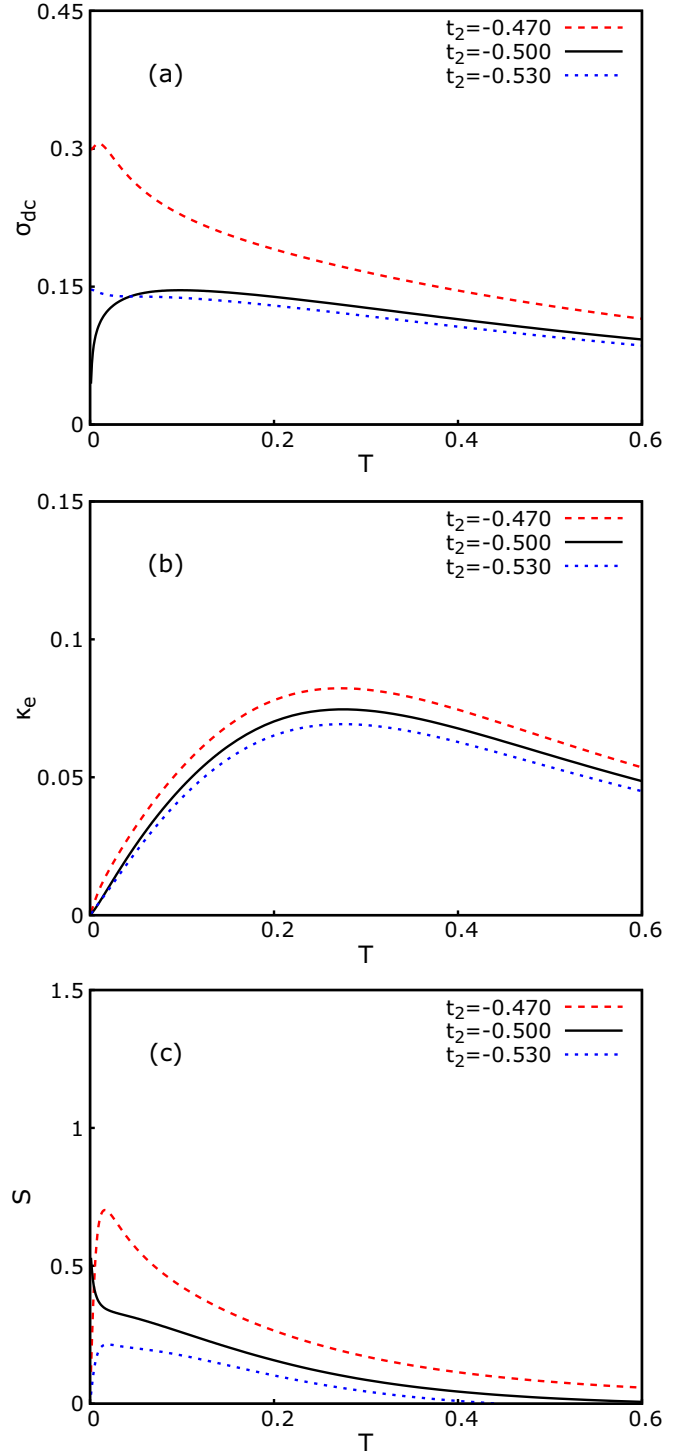


FIG. 8. Temperature dependences of the (a) dc conductivity σ_{dc} , (b) thermal conductivity κ_e , and (c) Seebeck coefficient S are shown for the same parameters as in Fig. 7.

positive t^{++} , as the resonant peak affects strongly the transport properties (see Fig. 10).

2. Strong-coupling regime

A large enough Coulomb interaction U leads to the reconstruction of the DOS and transport function. In the strong-coupling regime, a large Mott-Hubbard gap governs

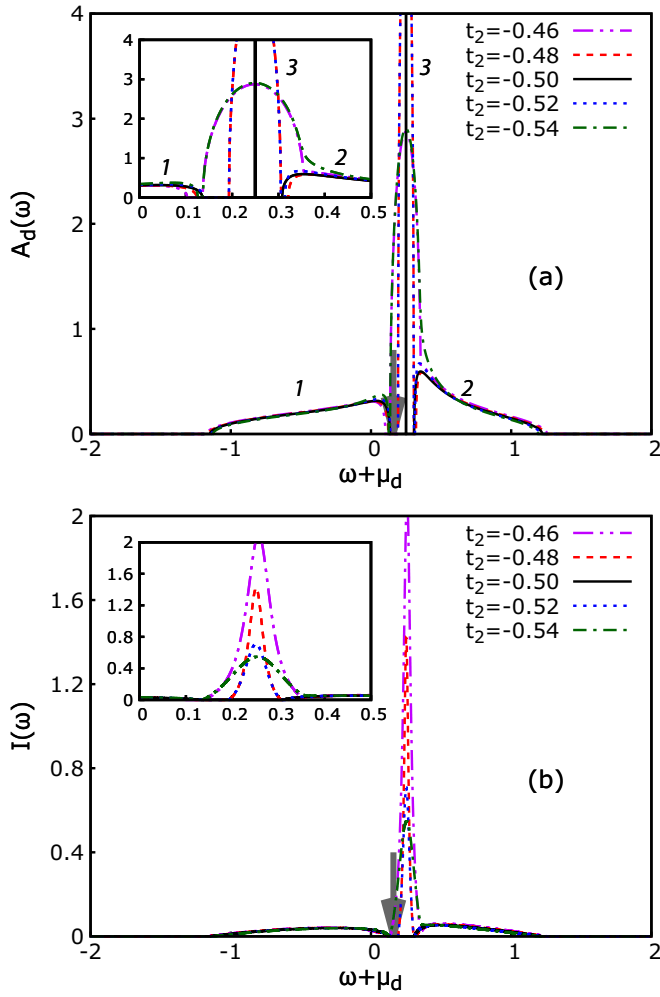


FIG. 9. The interacting DOS (panel a) and transport function (panel b) plotted versus ω for $U = 0.25$, $n_f = 0.75$, $n_d = 1 - n_f = 0.25$, and for $t_2 = -0.46, -0.48, -0.5, -0.52, -0.54$. Labels 1, 2, and 3 denote the lower Hubbard band, the upper Hubbard band, and band of localized states, respectively. The gray arrow indicates a narrow ω interval in which E_F is located for different values of t_2 .

the transport properties at low temperatures. Besides, the upper Hubbard band becomes narrow and acquires a high density of states.

At half filling and $t^{++} = 0$ ($t_2 = -0.5$), the upper Hubbard band has a singularity at the bottom edge, where the transport function shows only a steplike feature (see Fig. 11). The dc charge and thermal conductivities are similar to what one sees in doped Mott insulators [35,43,44], but the Seebeck coefficient is different: it is negative and displays anomalous behavior at low temperatures (see Fig. 12). Such a behavior is reflected in the anomalous temperature dependence of the chemical potential caused by the singularity in the DOS. For $t^{++} \neq 0$, the features in the upper Hubbard band are smoothed. For $t^{++} > 0$ ($t_2 > -0.5$), the resonant peak dominates the transport function, so that the dc charge and thermal conductivities increase, and the Seebeck coefficient is positive. The anomalous behavior is shifted to lower temperatures.

An increase of doping has a twofold effect. First, it expands the $\omega - t_2$ region in which the Mott gap is observed [see

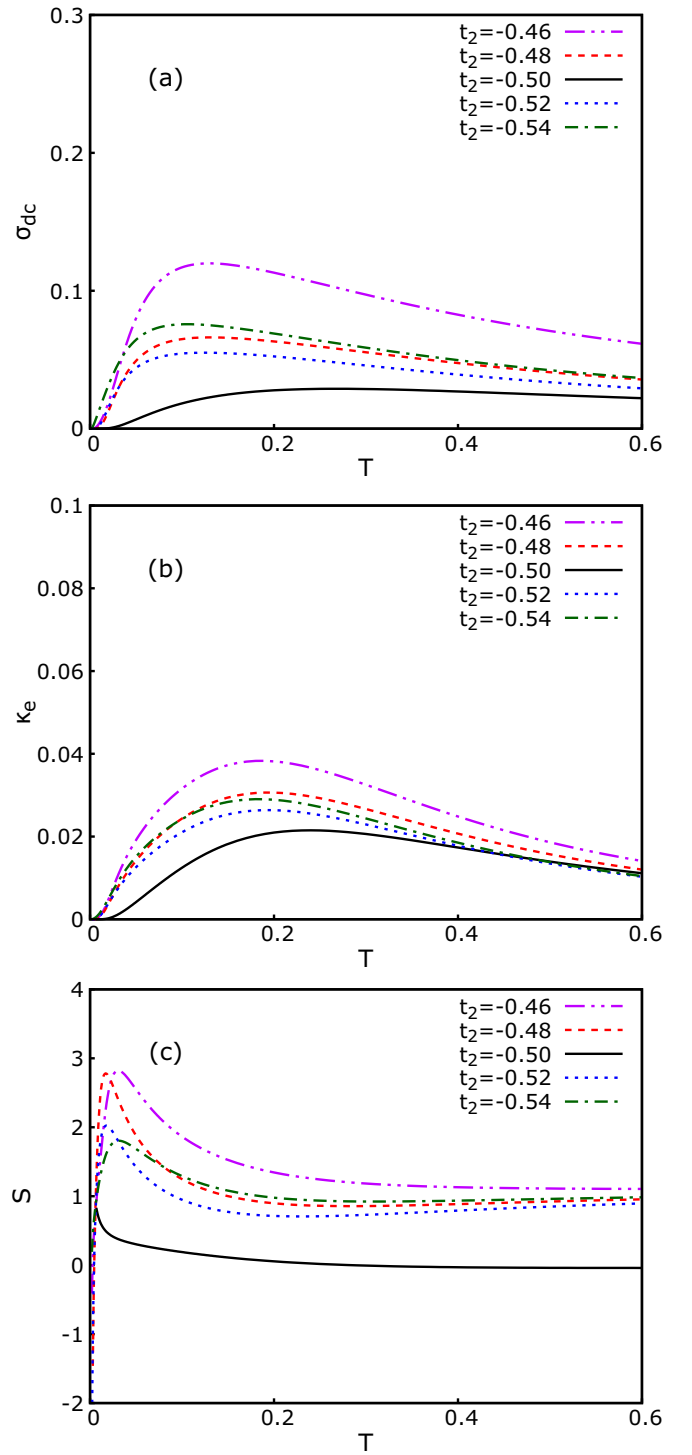


FIG. 10. Temperature dependence of the (a) dc conductivity σ_{dc} , (b) thermal conductivity κ_e , and (c) Seebeck coefficient S in the weak-coupling regime is shown for the same parameters as in Fig. 9.

panels (c) and (d) in Fig. 2]. Second, for t^{++} in a narrow interval around $t^{++} = 0$ ($t_2 = -0.5$), it leads to the three-band structure in the DOS and transport function. This is illustrated in Fig. 13(a), where the lines (1), (2), and (3) represent the lower Hubbard band, the upper Hubbard band, and the band of localized states, respectively. The δ peak in the DOS, observed

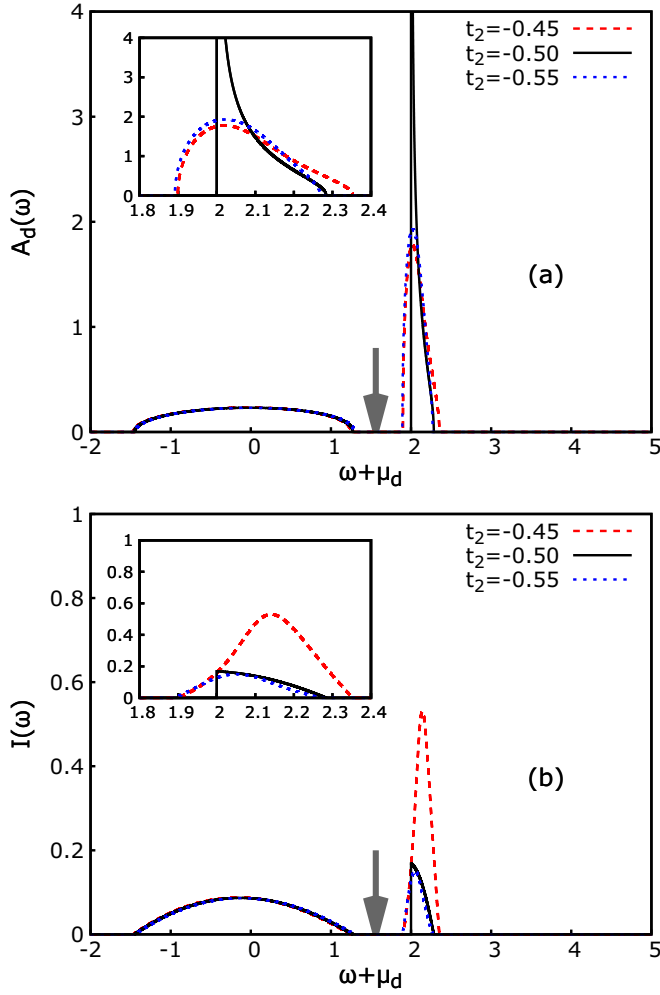


FIG. 11. The interacting DOS (panel a) and transport function (panel b) is plotted versus ω for $U = 2$ at half filling ($n_f = n_d = 1/2$) and for $t_2 = -0.45, -0.5, -0.55$ ($t_3 = 0$). The gray arrow indicates a narrow ω interval in which E_F is located for different values of t_2 .

for $t^{++} = 0$ exactly, is represented by the vertical line (3). This singular feature is coming from the localized d states and the corresponding singularity in the transport function is absent. Any deviation of t^{++} from zero broadens the δ peak into a narrow band of excitations which contribute to the heat and charge transport (see Fig. 14). For a sufficiently large value of $|t^{++}|$, the band of localized states [line (3) in Fig. 13] merges with the upper Hubbard band [line (2)] so that the sharp features in the DOS are smoothed out. In comparison with the half-filled case shown in Figs. 11 and 12, the Mott gap is now larger, so that we obtain smaller values of the dc charge and thermal conductivities, and the Seebeck coefficient, for t^{++} close to zero. For larger values of $|t^{++}|$, the resonant peak dominates the transport function, which becomes large for positive t^{++} ($t_2 > -0.5$) and relatively small for negative t^{++} ($t_2 < -0.5$), so that the dc charge and thermal conductivities increase. The comparison with the undoped case shows that the temperature dependence of the Seebeck coefficient is modified and $S(T)$ is now larger and positive.

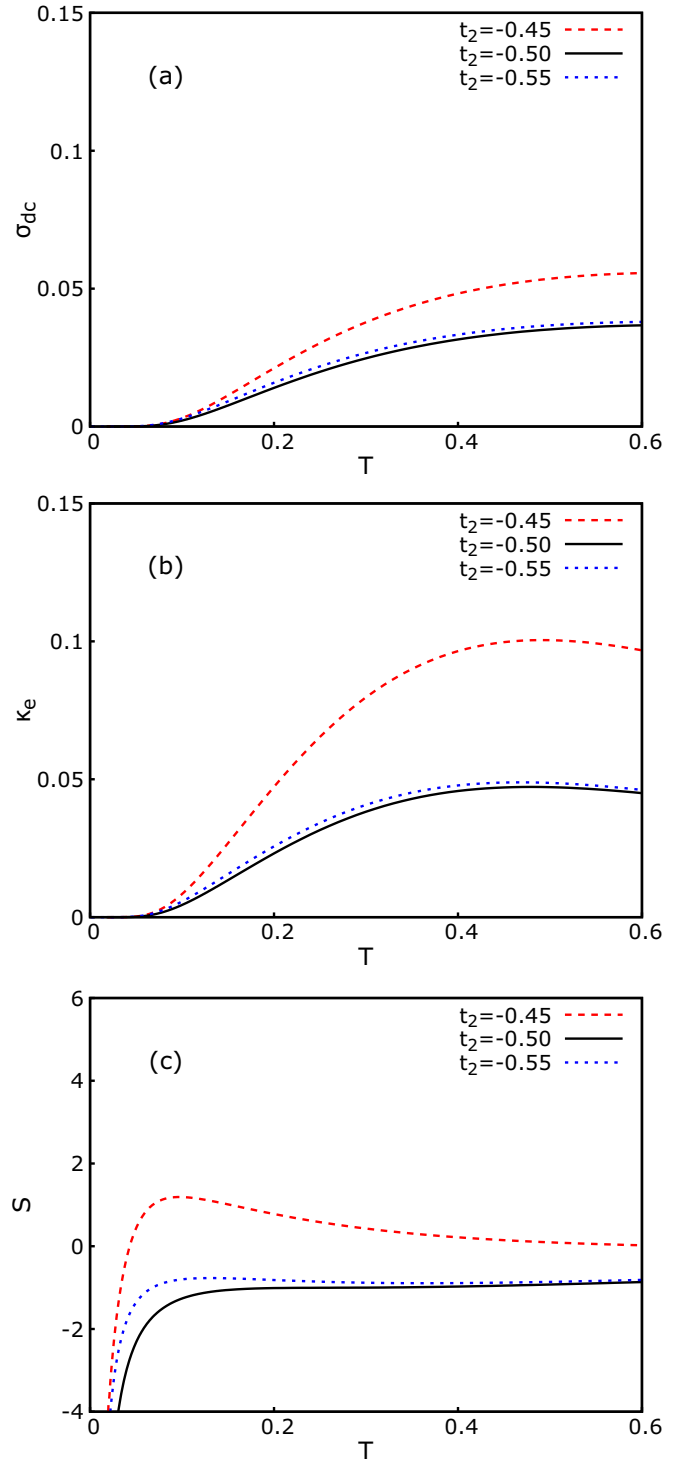


FIG. 12. Temperature dependence of the dc conductivity σ_{dc} , the thermal conductivity κ_e , and Seebeck coefficient S in the strong-coupling regime is shown for the same parameters as in Fig. 11.

V. DISCUSSION AND CONCLUSIONS

In this article we studied the effects of correlated hopping on the density of states and transport coefficients of the Falicov-Kimball model on a Bethe lattice with a semielliptic DOS.

Using dynamical mean-field theory, we derived an exact solution for the renormalized DOS $A_d(\omega)$ and the transport

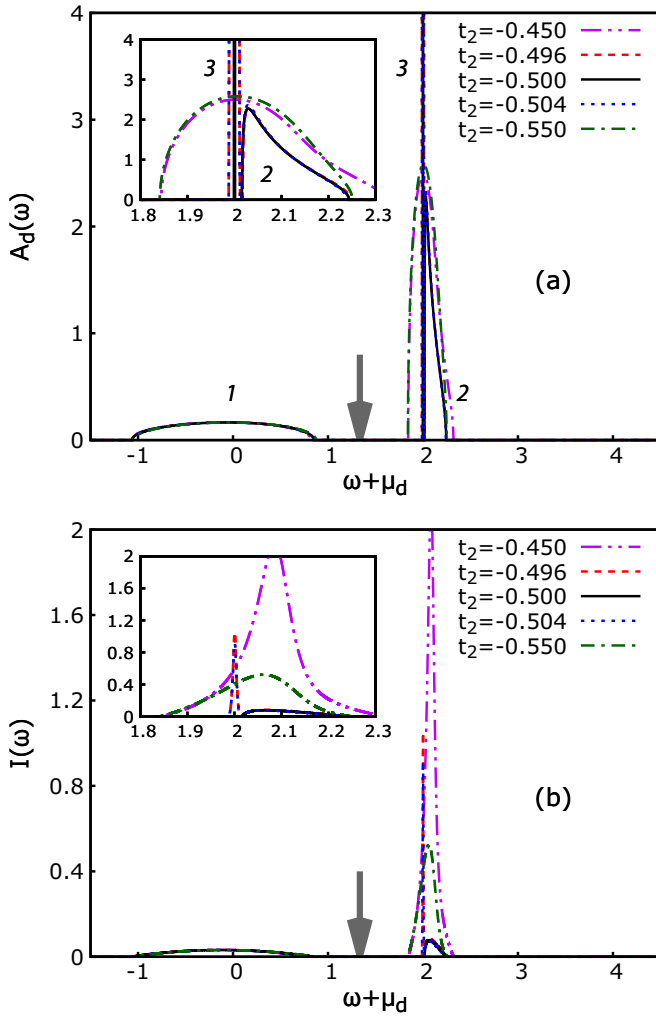


FIG. 13. The interacting DOS (panel a) and transport function (panel b) for $U = 2$ and $n_f = 0.75$, and $n_d = 1 - n_f = 0.25$. Here, $t_2 = -0.45, -0.496, -0.5, -0.504, -0.55$ and labels 1, 2, and 3 denote the lower Hubbard band, the upper Hubbard band, and the band of localized states, respectively. The gray arrow indicates a narrow ω interval in which E_F is located for different values of t_2 .

function $I(\omega)$, and computed the transport coefficients via the Boltzmann relations (Jonson-Mahan theorem). The bandwidth of $A_d(\omega)$ and $I(\omega)$ is found to be the same, but their functional form is completely different, showing that correlated hopping renormalizes the single-particle and the two-particle properties in a different way. As regards $A_d(\omega)$, the main effect of correlated hopping is an effective narrowing of the bandwidth, accompanied by the opening of a Mott-Hubbard gap and, at finite doping, the emergence of a band of localized states. As regards $I(\omega)$, its behavior is dominated by the resonant peak which appears in the region of the parameter space (small values of $|t^{++}|$), where the single-particle states are localized. Our interpretation of the resonance is that it manifests a two-particle interference in random media, e.g., weak (anti)localization [45]. The correlated hopping mimics the random media, with different values of the hopping integral corresponding to the random distances between the atoms. From this point of view, Eq. (45) is the interference condition for d particles following different trajectories over the lattice

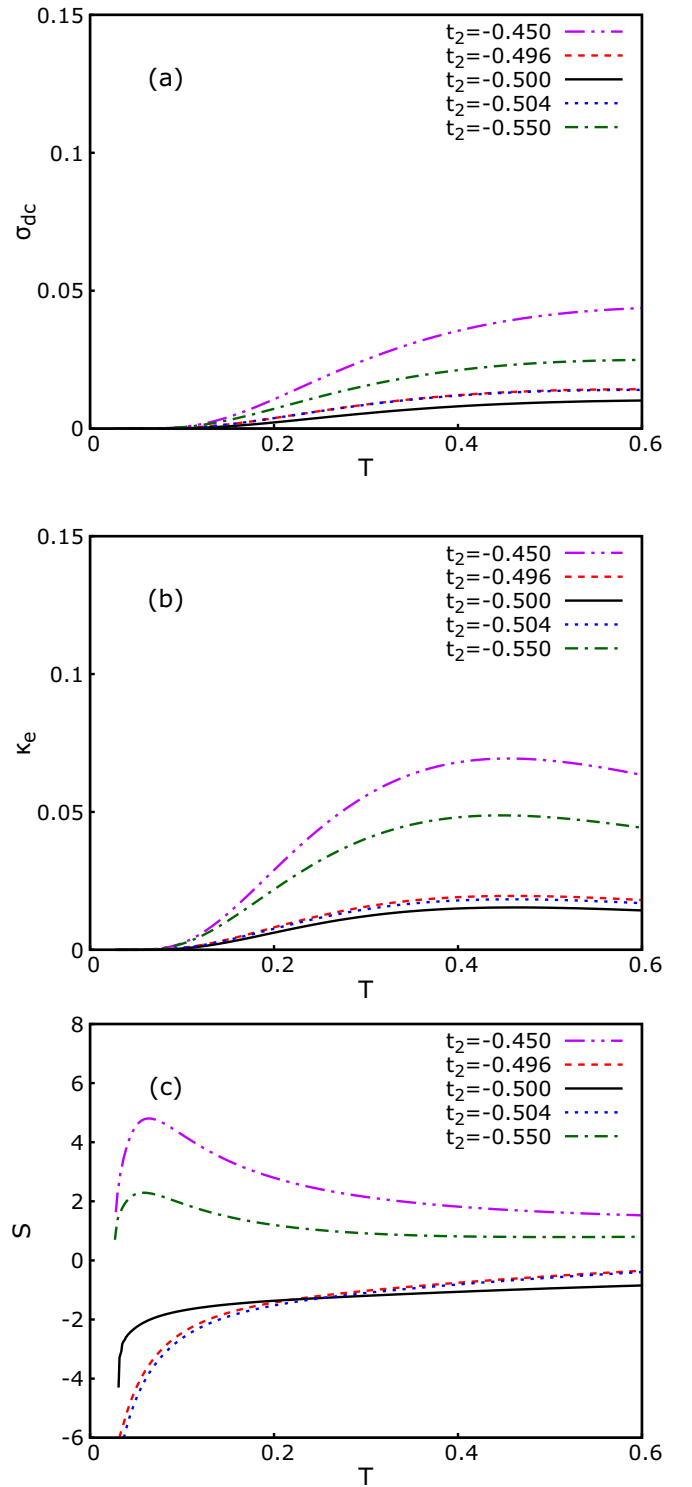


FIG. 14. Temperature dependence of the dc conductivity σ_{dc} , the thermal conductivity κ_e , and Seebeck coefficient S for the same parameters as in Fig. 13.

sites, which are either occupied or unoccupied by the f particles.

In our previous article [33] it was found that the charge and heat transport of particles described by the Falicov-Kimball model on a hypercubic lattice exhibits a number of surprising features. However, the anomalies were associated with the

peculiarities of the Gaussian density of states, which does not have the clear-cut band edge and has a finite “quasiparticle” scattering time for frequencies outside the band. To our surprise, similar behavior is obtained for a Bethe lattice with a semielliptic density of states, so that the anomalous transport coefficients seem to be a common feature of systems with correlated hopping.

The anomalous features of $I(\omega)$, due to the resonant two-particle contribution, are observed for a wide range of the correlated hopping parameter, t_2 . In this parameter range, the renormalized one-particle DOS does not display any anomalies. The analytic expression for the resonant frequency, given by Eq. (46), shows that by tuning the concentration of the itinerant electrons we can bring the Fermi level close to the resonance and increase substantially the conductivities and thermoelectric power.

The reduction of the amplitude of correlated hopping between the sites occupied by the f particles creates, for $t^{++} \rightarrow 0$, clusters of sites occupied by f electrons and the ensuing band of localized d states. When the f

electron concentration is above half filling, $n_f > 0.5$, this band can be seen in the single-particle DOS, in addition to the lower and upper Hubbard band. Depending on the concentration of d electrons, the Fermi level is either in the lower ($n_d < 1 - n_f$) or in the upper ($n_d > n_f$) Hubbard band or in the band of localized states ($1 - n_f < n_d < n_f$). In each of these cases, the thermoelectric coefficients exhibit completely different behaviors.

Finally, we remark that a large enhancement of the conductivities by correlated hopping, driven by the emergence of two-particle resonant states, has been found here for the Falicov-Kimball model with static interaction. It would be interesting to check whether similar transport anomalies emerge in the models with dynamic interactions, e.g., in the Hubbard model with correlated hopping.

ACKNOWLEDGMENTS

V.Z. acknowledges support by the Ministry of Science of Croatia under the bilateral agreement with the USA on scientific and technological cooperation, Project No. 1/2016.

-
- [1] J. Hubbard, Electron correlations in narrow energy bands, *Proc. R. Soc. London, Ser. A* **276**, 238 (1963).
 - [2] M. E. Foglio and L. M. Falicov, New approach to the theory of intermediate valence, I. General formulation, *Phys. Rev. B* **20**, 4554 (1979).
 - [3] M. E. Simón and A. A. Aligia, Brinkman-Rice transition in layered perovskites, *Phys. Rev. B* **48**, 7471 (1993).
 - [4] J. A. Blackman, D. M. Esterling, and N. F. Berk, Generalized locator, Coherent-potential approach to binary alloys, *Phys. Rev. B* **4**, 2412 (1971).
 - [5] J. E. Hirsch, Bond-charge repulsion and hole superconductivity, *Phys. C (Amsterdam, Neth.)* **158**, 326 (1989).
 - [6] B. R. Bulka, Superconductivity in the Hubbard model with correlated hopping: Slave-boson study, *Phys. Rev. B* **57**, 10303 (1998).
 - [7] L. Arrachea, E. R. Gagliano, and A. A. Aligia, Ground-state phase diagram of an extended Hubbard chain with correlated hopping at half-filling, *Phys. Rev. B* **55**, 1173 (1997).
 - [8] M. Tsuchiizu, Y. Omori, Y. Suzumura, M.-L. Bonnet, and V. Robert, Ab initio derivation of multi-orbital extended Hubbard model for molecular crystals, *J. Chem. Phys.* **136**, 044519 (2012).
 - [9] L. Didukh, Yu. Skorenky, Yu. Dovhopyaty, and V. Hankevych, Metal-insulator transition in a doubly orbitally degenerate model with correlated hopping, *Phys. Rev. B* **61**, 7893 (2000).
 - [10] M. Kollar and D. Vollhardt, Correlated hopping of electrons: Effect on the Brinkman-Rice transition and the stability of metallic ferromagnetism, *Phys. Rev. B* **63**, 045107 (2001).
 - [11] Y. Meir, K. Hirose, and N. S. Wingreen, Kondo Model for the “0.7 Anomaly” in Transport through a Quantum Point Contact, *Phys. Rev. Lett.* **89**, 196802 (2002).
 - [12] A. Hübsch, J. C. Lin, J. Pan, and D. L. Cox, Correlated Hybridization in Transition-Metal Complexes, *Phys. Rev. Lett.* **96**, 196401 (2006).
 - [13] S. B. Tooski, A. Ramšak, B. R. Bulka, and R. Žitko, Effect of assisted hopping on thermopower in an interacting quantum dot, *New J. Phys.* **16**, 055001 (2014).
 - [14] O. Jürgensen, K. Sengstock, and D.-S. Lühmann, Density-induced processes in quantum gas mixtures in optical lattices, *Phys. Rev. A* **86**, 043623 (2012).
 - [15] M. Di Liberto, C. E. Creffield, G. I. Japaridze, and C. Morais Smith, Quantum simulation of correlated-hopping models with fermions in optical lattices, *Phys. Rev. A* **89**, 013624 (2014).
 - [16] M. Eckholt and J. J. García-Ripoll, Correlated hopping of bosonic atoms induced by optical lattices, *New J. Phys.* **11**, 093028 (2009).
 - [17] D.-S. Lühmann, O. Jürgensen, and K. Sengstock, Multi-orbital and density-induced tunneling of bosons in optical lattices, *New J. Phys.* **14**, 033021 (2012).
 - [18] O. Jürgensen, F. Meinert, M. J. Mark, H.-C. Nägerl, and D.-S. Lühmann, Observation of Density-Induced Tunneling, *Phys. Rev. Lett.* **113**, 193003 (2014).
 - [19] L. M. Falicov and J. C. Kimball, Simple Model for Semiconductor-Metal Transitions: SmB_6 and Transition-Metal Oxides, *Phys. Rev. Lett.* **22**, 997 (1969).
 - [20] Z. Gajek and R. Lemański, Correlated hopping in the 1d Falicov-Kimball model, *Acta Phys. Pol. B* **32**, 3473 (2001).
 - [21] J. Wojtkiewicz and R. Lemański, Ground states of the Falicov-Kimball model with correlated hopping, *Phys. Rev. B* **64**, 233103 (2001).
 - [22] J. Wojtkiewicz and R. Lemański, 2d Falicov-Kimball model with correlated hopping in the large U limit, *Acta Phys. Pol. B* **32**, 3467 (2001).
 - [23] H. Čenčariková and P. Farkašovský, Formation of charge and spin ordering in strongly correlated electron systems, *Condens. Matter Phys.* **14**, 42701 (2011).
 - [24] W. Metzner and D. Vollhardt, Correlated Lattice Fermions in $d = \infty$ Dimensions, *Phys. Rev. Lett.* **62**, 324 (1989).
 - [25] U. Brandt and C. Mielsch, Thermodynamics and correlation functions of the Falicov-Kimball model in large dimensions, *Z. Phys. B: Condens. Matter* **75**, 365 (1989).
 - [26] A. Georges, G. Kotliar, W. Krauth, and M. J. Rozenberg, Dynamical mean-field theory of strongly correlated fermion

- systems and the limit of infinite dimensions, *Rev. Mod. Phys.* **68**, 13 (1996).
- [27] J. K. Freericks and V. Zlatić, Exact dynamical mean-field theory of the Falicov-Kimball model, *Rev. Mod. Phys.* **75**, 1333 (2003).
- [28] A. Schiller, Correlated hopping in the Falicov-Kimball model: A large-dimensions study, *Phys. Rev. B* **60**, 15660 (1999).
- [29] A. M. Shvaika, Dynamical mean-field theory of correlated hopping: A rigorous local approach, *Phys. Rev. B* **67**, 075101 (2003).
- [30] A. M. Shvaika, Erratum: Dynamical mean-field theory of correlated hopping: A rigorous local approach [*Phys. Rev. B* **67**, 075101 (2003)], *Phys. Rev. B* **82**, 119901(E) (2010).
- [31] K. Hoshino and K. Niizeki, The CPA calculation of the thermoelectric power of a binary alloy with off-diagonal disorder, *J. Phys. Soc. Jpn.* **38**, 1320 (1975).
- [32] H. Shiba, A reformulation of the coherent potential approximation and its applications, *Prog. Theor. Phys.* **46**, 77 (1971).
- [33] A. M. Shvaika, Effect of correlated hopping on thermoelectric properties: Exact solutions for the Falicov-Kimball model, *Condens. Matter Phys.* **17**, 43704 (2014).
- [34] J. K. Freericks, D. O. Demchenko, A. V. Joura, and V. Zlatić, Optimizing thermal transport in the Falicov-Kimball model: The binary-alloy picture, *Phys. Rev. B* **68**, 195120 (2003).
- [35] A. V. Joura, D. O. Demchenko, and J. K. Freericks, Thermal transport in the Falicov-Kimball model on a Bethe lattice, *Phys. Rev. B* **69**, 165105 (2004).
- [36] J. K. Freericks and R. Lemański, Segregation and charge-density-wave order in the spinless Falicov-Kimball model, *Phys. Rev. B* **61**, 13438 (2000).
- [37] W. Metzner, Linked-cluster expansion around the atomic limit of the Hubbard model, *Phys. Rev. B* **43**, 8549 (1991).
- [38] M. Jonson and G. D. Mahan, Mott's formula for the thermopower and the Wiedemann-Franz law, *Phys. Rev. B* **21**, 4223 (1980).
- [39] M. Jonson and G. D. Mahan, Electron-phonon contribution to the thermopower of metals, *Phys. Rev. B* **42**, 9350 (1990).
- [40] J. K. Freericks, V. Zlatić, and A. M. Shvaika, Electronic thermal transport in strongly correlated multilayered nanostructures, *Phys. Rev. B* **75**, 035133 (2007).
- [41] L.-F. Arsenault and A.-M. S. Tremblay, Transport functions for hypercubic and Bethe lattices, *Phys. Rev. B* **88**, 205109 (2013).
- [42] W. Chung and J. K. Freericks, Charge-transfer metal-insulator transitions in the spin- $\frac{1}{2}$ Falicov-Kimball model, *Phys. Rev. B* **57**, 11955 (1998).
- [43] V. Zlatić and J. K. Freericks, Strongly Enhanced Thermal Transport in a Lightly Doped Mott Insulator at Low Temperature, *Phys. Rev. Lett.* **109**, 266601 (2012).
- [44] V. Zlatić, G. R. Boyd, and J. K. Freericks, Universal thermopower of bad metals, *Phys. Rev. B* **89**, 155101 (2014).
- [45] G. Bergmann, Physical interpretation of weak localization: A time-of-flight experiment with conduction electrons, *Phys. Rev. B* **28**, 2914 (1983).